A NOVEL POWERED TWO-WHEELER RIDER DUMMY; SPECIFICATIONS AND INITIAL TESTING

Jolyon Carroll
Autoliv Research
Sweden

Bernard Been
Mark Burleigh
Humanetics
The Netherlands and UK, respectively

Paper Number 23-0132

ABSTRACT

Powered Two and Three-Wheelers (PTWs) are a popular means of transport. Fully electric PTWs can be operated locally emission-free and, therefore, may support sustainable transport options. However, in terms of the safety offered to PTW riders there is still a long way to go compared with other means of transportation. As such, PTW riders are a vulnerable road user group that stands to benefit from improved protection. Primarily, this paper provides a detailed description of the work-in-progress regarding a new crash test dummy, an ATD (Anthropometric Test Device), intended principally for use in testing PTWs. The question posed was if a new dummy can facilitate evaluations of PTW protective systems. The end goal being to promote more widespread evaluation of protective systems for PTW riders. Importantly, the development of the PTW riding dummy has paired physical and finite element models together, from the start, to support both physical and virtual testing in the future.

The ATD development is based on collision (and injury) statistics of PTWs worldwide, a brief summary of previous research is presented. As with the development of the Motorcyclist Anthropometric Test Device (MATD- ISO 13232-3) an updated modification of the Hybrid III pedestrian is proposed as the principal solution. To this base dummy a small set of modifications are made to allow simple and yet adequate representation of a PTW rider. Demonstration of the dummy in use as a PTW rider is provided by performing full-scale crash tests. Finite element crash simulations are compared with the physical tests, demonstrating the suitability of using the finite element dummy model in virtual PTW tests.

Details of the PTW dummy anthropometry are provided as well as the rationale for design updates in comparison with the MATD.

An overview of testing with the dummy is provided and the results from two full-scale reference tests (without protective system) are given. Injury predictions based on dummy measurements are compared with an injury statistics summary.

Differences between the outputs from the physical and finite element models are discussed in the context of the injury statistics and additional validation of the tools is suggested. The paper also indicates potential areas where the dummy could be improved in the future, depending on injury prediction needs and application, such as to include additional instrumentation in the abdomen region, for example.

Worldwide road traffic statistics suggest that the number of deaths of PTW riders form an equally large group as deaths among drivers and passenger of four-wheeled vehicles. In contrast, the former group has not benefitted from the advancement of protection systems as implemented in the latter. The availability of new tools in the form of a hardware ATD and its finite element model representing the PTW rider, will support development and evaluation of protective systems for PTW riders.

INTRODUCTION

Increasing numbers of people in both developed and low- and middle-income countries are choosing to use Powered Two-Wheelers (PTWs) [1]. Correspondingly, nearly 30% of all crash fatalities reported to WHO (World Health Organization) in 2016 involve PTWs, such as motorcycles, mopeds, scooters, and electrical bikes (e-bikes) [2] and this percentage has been increasing [3].

To combat this trend of increasing casualties, certain road safety interventions specific to PTW safety are accepted as being effective, such as: segregated lanes [4], motorcycle antilock braking systems [5] and the introduction of compulsory training and a skills test to obtain a motorcycle permit or licence [6]. However, without universal implementation and application of these and other known and future preventative solutions, crashes will still occur, and protective countermeasures remain crucial, such as the wearing of a motorcycle helmet [7].

It is more than 40 years since conclusions called for radical design changes to the motorcycle and the clothing of the rider as the only ways of increasing the chances of survival for the rider in high-speed impacts [8]. It is also more than 40 years since energy absorbers on the front of motorcycles, restraining chest pads, airbags and leg protectors have been proposed for motorcycle applications [9]. However, despite the potential benefits shown in research, only an airbag system survived, in a recognisable form, to a modern motorcycle [10].

To facilitate the common evaluation of secondary safety devices on PTWs, ISO 13232 was developed [11]. This standard makes use of the Motorcycle Anthropometric Test Device (MATD) [12]. ISO 13232 is not a safety standard or explicit legal requirement, but provides a methodology by which assertions regarding safety efficacy of proposed devices needs to be evaluated to be accepted by the scientific community [13]. After release of the standard in 1996, the cost of specific motorcycle dummies was already cited as a barrier to testing by 1998 [14]. As a result, Berg et al. and other authors after them choose to use the baseline Hybrid III crash dummy instead of the MATD negating the potential advantages of a bespoke dummy for PTW testing.

To return to, and to accelerate the evaluation of protective systems for PTW riders, a new initiative sought to develop a small set of modifications to the Hybrid III 50th percentile male crash test dummy. These were intended to capture useful features for PTW crash test applications and help proliferate availability of a dummy suitable for use beyond the research domain (i.e., entering system development and potentially even third-party evaluations).

This paper provides details of the resulting PTW riding dummy (PTW dummy). This includes its anthropometry as well as the rationale for design updates in comparison with the MATD. Results from two full-scale reference tests (without protective system) are given. The discussion compares injury predictions based on dummy measurements with expectations from the injury statistics summary. Differences between the outputs from the physical and finite element models are discussed, qualitatively, and additional validation of the tools is suggested.

Collision data direction

In 1981 a benchmark was set for motorcycle accident investigation in Southern California [15]. Data from 900 on-scene, in-depth cases were analysed with regard to injury causes. This evidence later formed a substantial part of the basis for the ISO Standard (13232) and the collision configurations most commonly encountered were encapsulated in the recommended test conditions. There were contemporary, in-depth studies in European countries too, some of which have continued. Five samples, from France, Germany, Netherlands, Spain, and Italy were brought together for the MAIDS research project (In-depth investigations of accidents involving powered two wheelers) [16]. This European PTW collision data of 921 investigations again indicated that the object most frequently struck was a passenger car. However, the frequency with which different configurations occurred varied between the U.S., German (ISO data) and the aggregated European (MAIDS) data [17]. Nevertheless, it was maintained that development and testing of protective devices should use a set of impact conditions including: the PTW impacting the side of the car, head-on impacts, the car impacting the side of the PTW and rear-end impacts.

Across all crash configurations, the three most frequently injured body regions are the same for ISO13232 and MAIDS (Table 1), though the order changes.

Table 1.
Three most frequently injured body regions in PTW crashes [17].

Body region injuries (as a percentage)	ISO 13232	MAIDS
Head	6.6	5.0
Lower legs	5.1	8.0
Upper extremities and shoulders	3.9	9.4

The European Horizon 2020 project PIONEERS subsequently identified key accident scenarios in Europe [18]. In the Pioneers dataset neck, upper extremities, chest, spine, and pelvis all showed a higher injury frequency than those in the ISO 13232.

Country-to-country crash configuration differences were again highlighted with respect to in-depth collision data for Germany, China, and India [19]. In that study the German data indicated a priority with respect to the front of the PTW colliding with the side of the car. Here it can be noted that the impact angle was not always 90 degrees, and the impact position was often in front of the passenger compartment; though an image depicting a 90 degree PTW to passenger compartment of a car is shown in that paper alongside this most frequent configuration (which could be slightly misleading to the variability of angles and positions).

The distribution of injuries by AIS (Abbreviated Injury Scale) [20] body region points towards the extremities and the head being priorities at the AIS2+ (at least moderate) severity and the thorax replacing the upper extremities for AIS3+ (at least serious) injuries [21]. Particularly, for all PTW crashes, the most frequent AIS3+ injuries are femur fracture, rib cage fracture, lung injury, tibia fracture and cerebrum injury.

A difference in injury priorities has been shown depending on the type of PTW [22]. Although, quite similarly to the complete sample, for all PTW crashes where the PTW was a motorcycle (not a scooter), the most frequent AIS3+ injuries are femur fracture, rib cage fracture, tibia fracture, lung injury and fracture to the base of the skull. At the AIS2+ level the equivalent priorities in motorcycle crashes are cerebral concussion, tibia fracture, radius fracture, femur fracture and a vertebral injury.

Throughout all these studies, head and extremity injuries still represent a prime focus for prevention, along with the ribs and lungs for severe cases.

RATIONALE FOR THE PTW RIDER DUMMY

General description

The development of the PTW started with a short-list of requirements and reviewing the MATD features. Candidate dummies that could be used as a platform for the PTW needed to be robust and demonstrate well know performance. Further key features are the availability of spare parts and support, a well-validated CAE (computer-aided engineering) model and known and accepted injury measurements and reference scales. Various candidate dummies were considered (primarily frontal impact dummies for frontal PTW crash applications) such as: the Hybrid III, the THOR, and the Hybrid III pedestrian dummy with standing pelvis. The standard Hybrid III and THOR 50th percentile male dummies were not considered adequate because of their limitations to adapt to PTW sitting postures in the pelvis area, although the Hybrid III was scoring well on all other requirements. The THOR was not further considered because of its complexity and costs, having many features not relevant to PTW loading cases, and was also considered to be less robust.

Anthropometry

The PTW rider anthropometry is based on the RAMSIS Motorbike Posture Models ‘All-rounder’ and ‘Scooter’ [23]. RAMSIS is an ergonomics software tool used for vehicle cabin and workspace design. The motorbike posture models were based on previous experiments involving female and male volunteers sitting on scooters and allrounder motorcycles. Therefore the 50th percentile male rider postures were derived from volunteer data, using a human

anthropometry database and ergonomic posture prediction algorithms implemented in the RAMSIS software. The outputs of the RAMSIS models are both the external surface geometry, as well as the 'stickman' coordinates of joint positions in 3D space. The rider posture models were compared with the UMTRI (University of Michigan Transportation Research Institute) Anthropometry of Motor Vehicle Occupants (AMVO) data set [24] [25]. It was found that, after coordinate system transformation, the RAMSIS and AMVO stickmen correlated well for spinal curvature and length between the hip joint up to the occipital condyle joint for the allrounder (Figure 1), although the spine coordinates do not match exactly in between (e.g. from the AMVO point 60 to 57). The scooter posture matched well up until the 4th thoracic vertebra and shoulder height, with more deviations higher up. This study revealed that the spinal curvatures of scooter, allrounder and automotive seated postures are close up to the 4th thoracic vertebra. It seems likely that riders (and drivers) adapt their spinal postures based on the arm length and distance to the handlebars (steering wheel). Likely the spine and neck curvatures above the shoulder joints are adapting to keep the head in the desired angle for good vision and neck curvature adapts for least muscle effort to keep the helmeted head in the desired orientation.

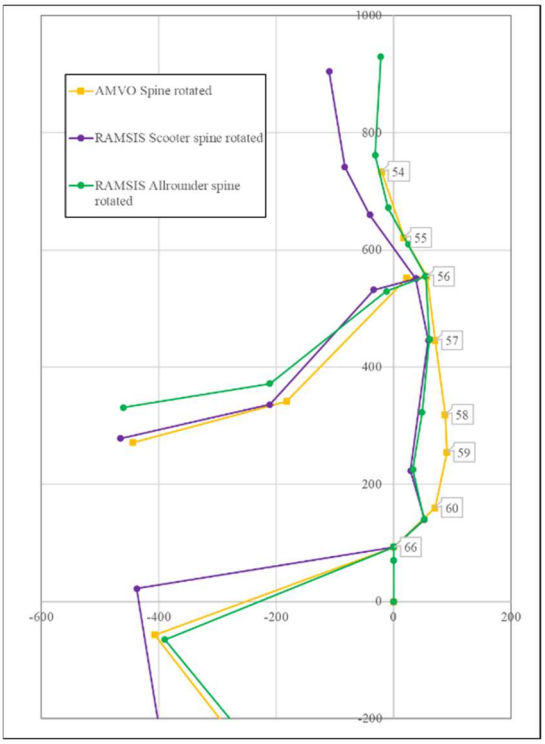

Figure 1. Overlay of AMVO, RAMSIS Scooter and Allrounder stickmen (with AMVO joint numbers: *66 = Hip [h-point]; 60 = L5/S1; 57 = T8/T9; 56 = T4/T5; 54 = Head/Neck [occipital condyle]**).***

TEST METHOD

Crash-Testing

To evaluate overall dummy behaviour, two crash tests were performed. In agreement with the most common scenario in Germany, these crashes involved the front of the PTW striking the side of a car. The two variations investigated were either a moving PTW to moving car or a moving PTW to stationary car. In both cases the speed of the PTW was nominally 50 km/h [19]. Just a little faster than the 48 km/h used in the ISO standard test requirements. Although, in the stationary car test a speed of only 48.7 km/h was achieved. When moving, the speed of the car was 20 km/h.

The loading to the body of the PTW rider could be different depending on where the PTW contacts the car. For the tests reported here, it was selected to strike the side of the car's passenger compartment. The intention was that by having an initial point of contact on the B-pillar of the car, then the rider could interact with this stiff structure and, potentially, have head contact with the roof-rail of the car.

For the car, a Honda Accord from 2011 was selected. As a 4-door midsize sedan, it has the body of a typical family car and a closely related finite element model available for use in corresponding simulation efforts [26]. A simplified version of this model was used for initial correlation work to reduce runtimes. Globally, bikes like the Honda CB 125 (and older CG 125) and Yamaha YS or YZ 125 have been market leaders. For this reason, previous research at Autoliv established a finite element model of a Yamaha YS125. Given the relevance of this bike size and type to the global markets, this was selected for the tests. A simulation model of this motorcycle was created at Autoliv prior to this study.

Launch mechanism The motorcycle was not linked directly to the test facility propulsion system, but indirectly accelerated up to speed via a supporting frame. The frame had two supporting tubes in line with the axle through the front wheel. It also provided stability for the rider under the arms and against the sides of the chest (Figure 2). The front wheel supporting tubes rotated and released the bike prior to the crash point so that the bike was clear of the frame and free-running momentarily before hitting the side of the car.

Figure 2. Rider and motorcycle within the frame used to accelerate and launch them to the crash point.

PTW RIDER DUMMY DESCRIPTION

Like the MATD, the PTW dummy is based on the Hybrid III 50th percentile male dummy with the pedestrian standing pelvis design. The pedestrian pelvis assembly is not restricting the legs in an automotive seating position, like the standard Hybrid III sitting pelvis does. It allows for a larger range of motion in the hip joints and enables the dummy to adapt to a range of rider postures seen on various PTW types. The pedestrian pelvis enables the legs to spread around a typical motorcycle tank. Moreover, the larger flexion and extension range of the hip joints allows the dummy to sit in more upright 'custom bike' and 'scooter' rider postures, as well as with more forward leaning and more flexed legs seen on sports bikes. Modifications to the Hybrid III dummy were implemented in the head & neck, the shoulder, the spinal column, and the pelvis.

PTW dummy features

For development of the dummy postures the RAMSIS models and anthropometry comparison provided good direction. It was concluded that the spine of the dummy could be kept the same for the scooter and allrounder models (Figure 3). The neck needs to be adjustable at its base and the OC-joint (occipital condyle) needs adaptation for head angles. The posture is also adjustable by the rocking of the pelvis which the standing pelvis allows. The shoulder joint position of the PTW rider is somewhat further forward, as compared to an automotive driver posture. A small adaptation in the Hybrid III shoulder components was found to be desirable (Figure 4). The Hybrid III thorax and spine were oriented to match the RAMSIS external surface and stickman, by implementing the pedestrian straight lumbar spine, a new interface bracket between the top of the lumbar and the thoracic spine, and a new adjustable neck bracket. A new sacrum block was also designed which incorporated a standard lumbar load cell.

The WorldSID head was chosen because of its human-like representation of the chin area for improved interaction with a helmet strap. The WorldSID neck was selected, as it is a good compromise demonstrating biofidelic performance in multiple directions: frontal flexion, oblique and lateral [27]. To adapt the head to a PTW rider vision

angle, the neck was modified with a set of bespoke buffers in the upper segment. The buffer set puts the top of the neck into 12 degrees more extension. The adjustable neck bracket is interfacing between the bottom of the WorldSID neck and the Hybrid III spine. The neck bracket provides fine adjustment of the head angle for the various rider postures between forward leaning sports posture (more extension) and relaxed custom rider posture (more flexion). A small modification was needed to fit the thoracic bib between the neck and the new bracket due to the neck moving rearward to match the RAMSIS stickman. The PTW dummy is using rigid knees (without knee sliders) for robustness. An exploded view of the bespoke PTW components is shown in Figure 5. Standard Hybrid III 50th percentile male parts are used to complete the PTW dummy assembly.

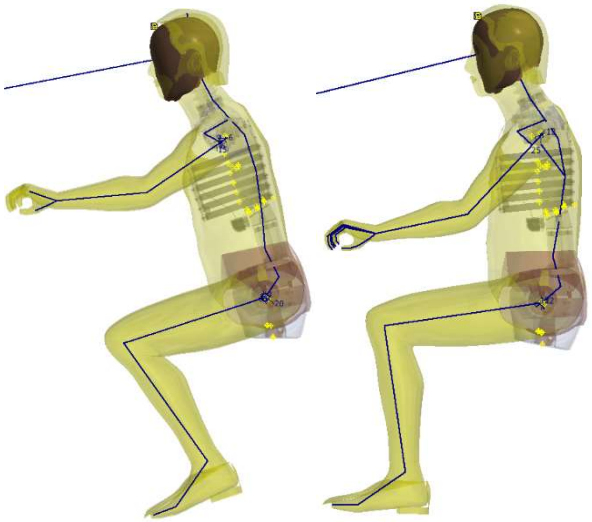

Figure 3. Overlays of the PTW dummy in two rider posture models allrounder (left image) and scooter (right image)

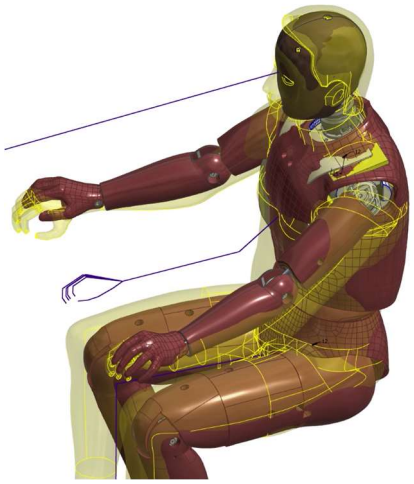

Figure 4. The PTW rider dummy CAD within RAMSIS allrounder external surface (note: only the left shoulder joint is modified to meet the PTW posture in this image to show the effect).

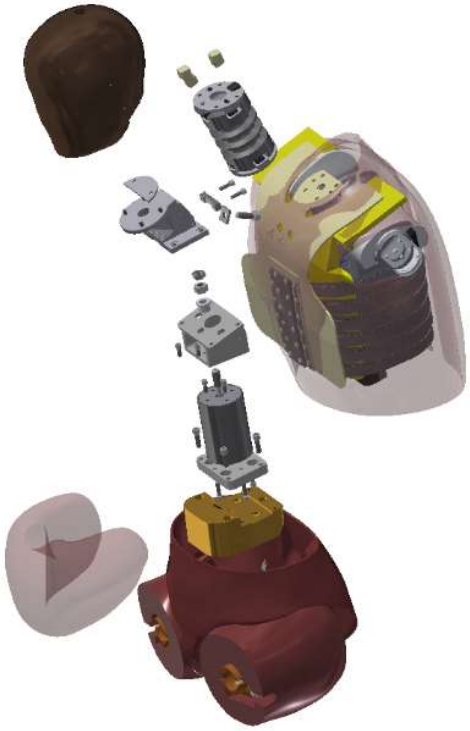

Figure 5. PTW rider dummy bespoke components (Use standard Hybrid III 50 parts to complete the assembly).

Instrumentation The PTW dummy adopted the Hybrid III 50th percentile arms and legs and so features standard options to add load cells in the humerus, the femur, and the tibia. In contrast to the MATD using frangible extremities, the load cells provide time histories of the loading, and data that can be reviewed to established injury criteria and human tolerances with adequate reproducibility. The dummy can be equipped with accelerometers and angular rate sensors in the major body segments, as well as tilt sensors to measure the dummy posture. Further load cells can be implemented in the head -to-neck -, the neck-to-upper spine - and lumbar-to-pelvis interfaces. The dummy is also equipped with the standard Hybrid III chest displacement sensor. Also, there is an option to equip the dummy with an on-board data acquisition system, to avoid cable damage in the, sometimes unpredictable, post-crash landing trajectory. For this testing, the PTW dummy was also equipped with the sensors described in Table 2.

Table 2.
Rider instrumentation

Region	**Instruments**
Head	3 axis linear accelerometer 3 x angular rate sensors
Helmet	3 axis linear accelerometer 3 x angular rate sensors
Upper neck	Load cell (measuring: 3 x forces and 3 x moments)
Chest	3 axis linear accelerometer Potentiometer (to give chest deflection)
Lumbar spine	Load cell (measuring: 2 x forces and 1 moment)
Pelvis	3 axis linear accelerometer
Femurs	Load cell (measuring axial force, 1 each side)

CAE model of the PTW dummy
Simultaneously with the physical dummy hardware engineering, a finite element dummy model (in LS-Dyna code) was developed (Figure 6) in two stages. Initially the first stage model was based on existing Hybrid III 50th percentile male dummy model finite element components. All the new PTW parts were meshed from CAD (computer-aided design) geometry, and relevant material models were adopted from the existing Hybrid III model material database. In the second stage the PTW dummy model was used in simulated test environments and conditions and validated against experimental data in the same test conditions. Material models and meshes were further fine-tuned and updated, until a satisfactory correlation was achieved between the experiment data and the CAE model response.

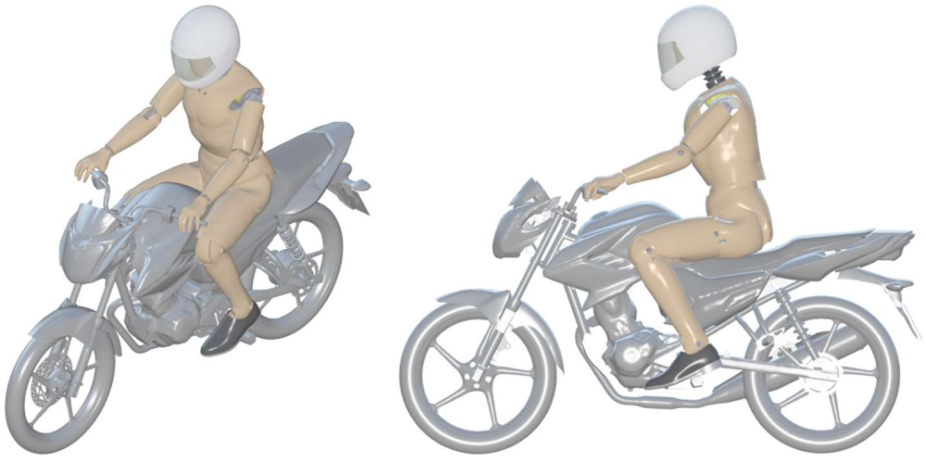

Figure 6. PTW dummy LS-Dyna model on the motorcycle model.

TEST RESULTS

Visual comparison

Visual comparisons of the motion are useful to appreciate the behaviour of the PTW dummy in these tests quickly. Still images from similar video views are provided in Figure 7 for the two physical tests.

For the first 20 milliseconds, there is little difference between the two tests. Distortion of motorcycle components is confined to the front wheel and mudguard. The rider maintains an upright sitting posture with head above the level of the car's roof rail. Then by 40 milliseconds, we see that the test with a stationary car keeps the front wheel of the motorcycle straight, whilst the moving car test begins to turn the front wheel to the right (away from the camera). The front fork is either deforming or turning and deforming. At 60 milliseconds, the rear wheel of the motorcycle lifts a little from the ground. This is more pronounced in the stationary car test and becomes even more obvious as the test progresses. At 80 milliseconds the handlebars of the motorcycle in the moving car test have turned and the change in motorcycle loading has already meant that the head of the rider is slightly closer to the car than in the stationary car test. Although in both tests the trajectory of the head towards the roof rail is now inevitable. At 100 milliseconds we are reaching the point of head contact in both tests. The lower legs of the PTW dummy in the stationary car test have swung forwards under their inertia. At 120 milliseconds it looks as though the body of the dummy is involved with neck loading, and the pelvis is higher in the stationary car test than in the moving car test. At 140 milliseconds the moving car test has produced more rotation of the helmet (and head within it) as it is pulled by the moving roof-rail. This sequence of still images concludes at 160 milliseconds, where the extent of the motorcycle yaw in the moving car test compared with pitch of the motorcycle in the stationary car test is most evident. The rear wheel of the motorcycle in the moving car test is back on the ground by this time.

Equivalent images comparing the physical with simulation stationary car test are available in Figure 9 in the Appendix. Comments on the moving car test are available already [28], although images from the moving car test and updated simulation are included in Figure 10. In both tests the simulations are in general agreement with the kinematics from physical tests. Although, the motorcycle showed more rebound after the initial contact with the car in the simulations compared with the physical tests. This resulted in the motorcycle leaping up off the ground. The deformation of the front wheel appears to be different, particularly in the stationary car setup and the compression and damping of the suspension in the front fork also appears to be different between physical and simulated crashes. The result for the rider is that the impulse coming through the motorcycle body and fuel tank will be different. Indeed, the virtual representation of the dummy lags behind the physical test kinematics. This is observable as the head contact time in the simulations which was, for example, 24 milliseconds later in the stationary car simulation than in the physical test.

Time (s)	Stationary car	Moving car
0.000		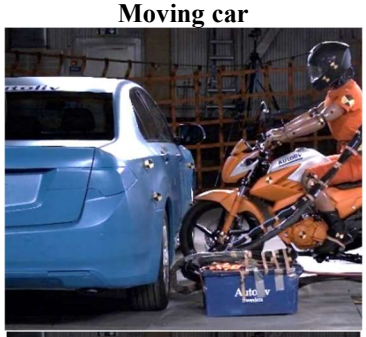
0.020		
0.040		
0.060		
0.080		

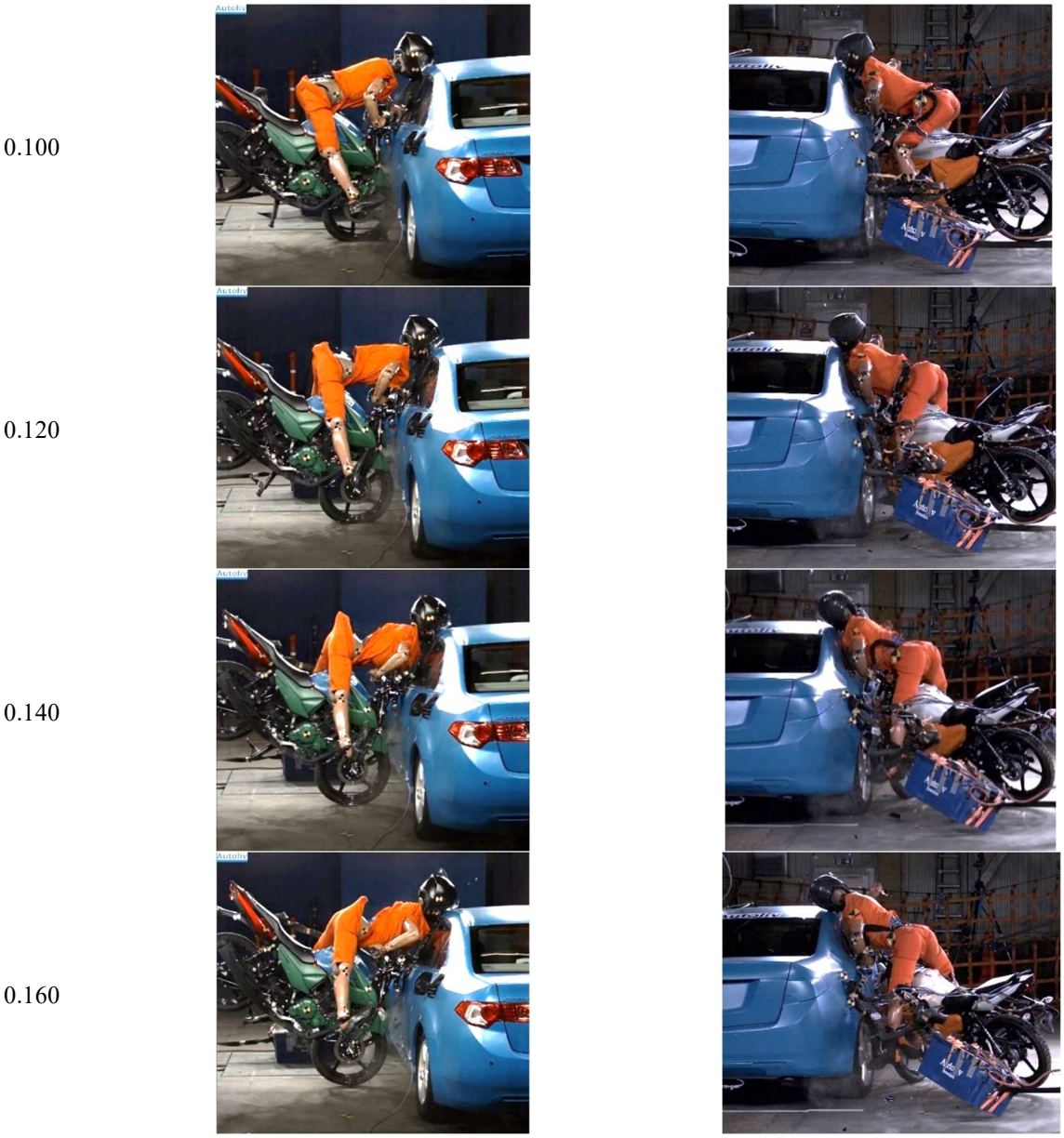

Figure 7. Still images from the video footage of two full-scale motorcycle to car crash tests. The left-hand column of images comes from the stationary car test and the right-hand column of images from the moving car test.

Dummy instrumentation

The instrumentation within the dummy is there to provide an assessment of the severity of loading to the rider. The peak values from some of the sensors are shown in Table 3. For priority metrics (relatable to injury predictions in the head, neck, thorax, and legs), these are matched with the equivalent peak from the virtual dummy in each case. Note that tensile femur forces are presented, rather than compressive as would often be referred to in car occupant protection scenarios, as the values for tension were higher than for compression.

Data were collected from the dummy without issue. Only one channel of data showed a fault, and that was the left femur load cell in the moving car test. Otherwise, the dummy and instrumentation were suitably robust, based on these two tests.

Table 3.
Peak values and selected injury criteria from the PTW dummy, resulting from two full-scale crash tests

Region	**Stationary car**		**Moving car**	
	Physical	Simulation	Physical	Simulation
Head – resultant linear acceleration (*g*)	567	490	209	291
Head – 3 ms exceedance (*g*)	123	196	161	83
HIC_{15}	6794	5827	2079	1471
Head – rotational velocity, y-axis (radian/s)	-33	-26	-42	-26
Head – rotational velocity, z-axis (radian/s)	6.5	2.9	39.8	10.9
Helmet – linear acceleration, x-axis (*g*)	-266		-166	
Helmet – rotational velocity, y-axis (radian/s)	+28.9 -22.6		+18.6 -40.8	
Upper neck - shear (N)	2937	4294	3365	4062
Upper neck – compression (N)	-5515	-9478	-1594	-1769
Upper neck – Moc-y (+flexion, -extension, Nm)	156 -48	124 -69	214 -58	241 -24
Chest - resultant linear acceleration (*g*)	40	58	66	37
Chest – deflection (mm)	4.6	3.0	6.2	3.6
Lumbar – z-axis (+tension, -compression, N)	+4185 -2005	+6132 -3747	+4292 -2697	+2904 -1973
Lumbar – y-axis moment (Nm)	-180	-166	-179	-136
Pelvis – resultant linear acceleration (*g*)	57	48	33	24
Femur – force (tensile, N)	3514 (right) 2856 (left)	2122 (right) 1677 (left)	1521 (right) †	978 (right) 600 (left)

† Left femur load cell failure

Alongside the dummy results, the motorcycle was examined after the test leading to certain qualitative observations, such as the deformation of the fuel tank (example in Figure 8). Work continues to create similar deformation patterns in the virtual fuel tank.

Figure 8. Images after the moving car test, showing the deformation of the fuel tank caused by the rider's pelvis.

DISCUSSION

Injury assessment

It is thought to be important to have a PTW contact with a moving collision partner as that relative motion will create yaw in the PTW and a twisting of the handlebars. These features will influence the PTW and rider motions and likely influence the design requirements for protective systems. The rider will not move straight forwards over the centre of the handlebars and engagement of the rider's legs with the handlebars and PTW structures will be biased towards one side. This behaviour was confirmed in these experiments.

In both moving and stationary car cases the dummy experienced a head contact (via the helmet) with the roof rail of the car. The helmet stayed on the head of the rider and the instrumentation within the head was useful to discern the difference between the moving car test and the stationary car test. It was observed that the moving car increased the head rotational metrics (particularly axial rotation) but decreased the linear, including the Head Injury Criterion. A HIC value of 2000 would give a 77% risk of a skull fracture [29] and confidently predict such an injury at 6000. Therefore, these tests provide useful load cases for assessing PTW head injury prevention countermeasures. The rotational velocities would also assess countermeasures intended to prevent concussions; the highest priority injury for PTW riders at the AIS2+ severity level. In that case, the moving car test would be a better representation of the challenges presented by the collision data, as the rotational velocities are higher than in the stationary car test.

The contact to the visor of the helmet is interesting and suggests a need to evaluate head protection in the face region. Full-scale tests are not expected to be ideal for controlled repetitive loading to a particular point on a helmet, but the helmet contact points in these two tests are remarkably similar. Helmet visor deformation was not observed in the simulations pointing towards a need for a more accurate representation of the helmet in future simulations.

The WorldSID neck was able to represent a realistic position of the rider's head with respect to viewing angle ahead of this motorcycle. Upper neck shear, compression, flexion, and extension were all close to levels where injuries to the neck (or base of the skull) could be expected with low but non-zero risk [30]. Neck injuries were not identified in the collision data as being a priority for PTW injury prevention. Therefore, we surmise that, the PTW dummy can position the head in an appropriate place, but it may need further work to understand how the neck loads relate to risk of injury for helmeted PTW riders.

Only limited loading of the chest and shoulders of the PTW dummy against the car was observed in this testing. The chest deflection measurements did not go above 6.2 mm. That corresponds with a negligible risk of serious injury [31]. This conflicts with rib cage fractures being a priority injury type for PTW riders, and with thoracic injuries being increasingly important as the severity of injury increases. Either the crash type is not representing the real-world conditions that create thoracic injuries (i.e., we have missed something in this experimental representation of typical events), or the PTW dummy kinematics created do not represent typical rider interactions, or the dummy chest design is not sensitive to the relevant deformation. It is suggested that, to some extent, all aspects are true though the balance of each is not known from this testing. Furthermore, some thoracic injuries are typically attributed to the ground contact in collision data and there remains the confounding factor that anterior to posterior chest deflection measurements may not be the most appropriate metric for predicting thoracic PTW rider injuries.

As of now, the PTW dummy possesses no possibility to measure abdominal loading. Whilst no clear abdomen penetration was observed in these two tests, the torso of the rider passes over the handlebars and there is potential for the rider's own PTW to cause loading to the abdomen in a slightly different collision or with a different PTW (e.g. a scooter, without prominent fuel tank). It is proposed that some abdomen instrumentation will be necessary in the development of protective countermeasures, and it is proposed that any such a modification to the dummy could also make a continuous frontal surface to the dummy without discontinuities between thorax and abdomen (i.e. to close the gap between the ribs and the abdomen insert – created when the Hybrid III adopts an upright posture).

In setting up equivalent simulation runs, it was evident that the dummy kinematics are influenced by the arm posture, interaction between pelvis and tank and even between foot and footrest. However, these parts in the PTW dummy are carried over directly from the base Hybrid III dummy. They have not been tuned for a PTW rider. Except for the frangible lower extremity bones and gripping hands, the same was true for the MATD, but perhaps those parts could have made a difference. Therefore, there remains an unanswered question as to whether it is important to model leg bone failure in order to represent accurately the behaviour of a PTW rider in a frontal crash. Certainly, the stationary car test generated tensile loading to the femurs; even if not compressive as could be the case

with direct loading to the knee, and at levels likely to be within tolerance limits so that fracture of the femur would not be expected on this input alone. It can be noted that there was little interaction between the PTW dummy and the handlebar in these tests. At the end of the moving car test sequence (Figure 10) the handlebar is over the femur of the rider furthest from the car and this shows how such an interaction could be important in a slightly different configuration with, for instance, earlier rotation of the handlebar or less pelvis restraint from the fuel tank.

The pelvis representation is a crucial factor in relation to three important aspects. The loading to the pelvis is enough to deform the fuel tank in these tests and quite probably create pelvis injury. This loading controls the subsequent kinematics of the rider and is, thus, important in the correct prediction of rider to opponent vehicle contacts. Also, that the force from the pelvis onto the fuel tank influences the motorcycle kinematics so that crash reconstructions looking at vehicle deformations and trajectories could be sensitive to the surrogate pelvis used. A pelvis angular rate sensor would at least help provide information about the interaction with the fuel tank and is recommended for an instrumentation update.

Physical and finite element model outputs

Unlike the physical crash, there was no relative movement in front fork components in these simulations. This absence of spring damper modelling is likely to be one of the reasons for generating a higher pitching angle in simulation than in the physical tests.

The front tyre also seemed to have a high stiffness, since the front wheel rebounded in the simulations once the initial contact with the car happens. Unlike the physical tests, there was no obvious deformation and compression in the base model of the motorcycle, so some alterations were made in generating the results presented here. However, this primary contact defines the main load path between the car and motorcycle, so there is a strong need to check the modified components and the accuracy of their representation in crash conditions.

The timing of helmet impact to the roof rail was delayed by 24 ms in the stationary car simulation compared with the physical test. Also, the timing of the contact between the front plastic components and the door was delayed by 10 ms in the simulation, when compared with the physical test. Both observations are also explainable given the potential lack of fidelity in the primary load path from the car side through the front wheel (and tyre) to the motorcycle frame and engine.

Observations on experimental setup

The experimental setup used for this testing was intended to replicate a typical path conflict, where a car turns across the path of a motorcycle, as seen around road junctions (intersections). It was not intended to recreate any specific rider reaction to the impending threat, though in many cases it seems possible that the rider could notice the conflict and may have time to brake before contact. Therefore, a limitation exists as the setup does not account for the braking response and muscle tensing of the rider. It also does not account, intentionally, for any pre-crash pitching of the motorcycle under emergency braking. However, whilst not planned, the physical representation of the intended setup does create some pre-crash pitching of the motorcycle. As the motorcycle front wheel is carried down the test track it is not rotating, but once released it touches the ground. The rotational inertia of the wheel gives a similar effect to braking and the motorcycle dives (pitches forward) during this free-running period prior to contact with the car. At present, this is a negative aspect of the testing, as it is difficult to recreate accurately in the simulations. In the future, this side effect could be useful if carefully designed to replicate a defined pre-crash braking behaviour. Otherwise, it may have to be removed with a setup modification if a truly non-braking response is desired.

CONCLUSIONS

Details of a PTW riding dummy are provided describing the tools and the rationale for necessary design updates over the base Hybrid III dummy. These include: the WorldSID head and neck, a new adjustable lower neck bracket, a rigid bracket at the top of the lumbar, the straight pedestrian lumbar spine plus the standing pelvis and thigh flesh components. The new PTW dummy exists physically as a prototype and as a finite element simulation model for CAE.

Both the physical and simulation versions of the PTW dummy have been tested in full-scale setups crashing a motorcycle into the side of a stationary or moving car. In both environments the testing concluded satisfactorily with data collected from the in-dummy instrumentation.

The motion of the simulated dummy differs from that observed in the physical test. However, this is not a criticism of the PTW dummy and dummy model as those differences appear to arise from the motorcycle model and from the motorcycle to car interaction. Nevertheless, the physical and simulation versions of the PTW dummy created head loading sufficiently high to generate reasonable risks of a head injury in the crashes. High femur loading was also present corresponding to the highest priority injuries based on the collision data for PTW crashes, albeit femur tension rather than compression.

The chest of the PTW dummy was not loaded severely in these tests, which raises a concern over the ability to investigate thoracic injury risk with this representation of a motorcycle front to car side crash. Both the chest and the pelvis of the dummy could be reviewed for biofidelity and injury prediction capabilities; though it is not yet clear what are the PTW rider-specific targets for these regions.

REFERENCES

[1] IMMA, "Safer Motorcycling - The Global Motorcycle Industry's Approach To Road Safety," International Motorcycle Manufacturers Association (IMMA), Genève, Switzerland, 2019.

[2] WHO, "Global status report on road safety 2018," World Health Organization (WHO), Geneva, 2018.

[3] WHO, "Powered two- and three-wheeler safety: a road safety manual for decision-makers and practitioners, second edition," World Health Organization (WHO), Geneva, 2022.

[4] R. U. R. Sohadi and M. a. H. B. Mackay, "Multivariate analysis of motorcycle accidents and the effects of exclusive motorcycle lanes in Malaysia," *Journal of Crash Prevention and Injury Control,* vol. 2, no. 1, pp. 11-17, 2000.

[5] E. R. Teoh, "Motorcycle antilock braking systems and fatal crash rates: updated results," *Traffic Injury Prevention,* vol. 23, no. 4, pp. 203-207, 2022.

[6] K. Kardamanidis, A. Martiniuk, R. Q. Ivers, M. R. Stevenson and K. Thistlethwaite, "Motorcycle rider training for the prevention of road traffic crashes," *Cochrane Database of Systematic Reviews,* vol. Art. No.: CD005240, no. 10, 2010.

[7] B. Liu, R. Ivers, R. Norton, S. Blows and S. K. Lo, "Helmets for preventing injury in motorcycle riders," *Cochrane database of systematic reviews,* vol. 4, pp. 1-42, 2009.

[8] J. Whitaker, "A survey of motorcycle accidents," Transport and Road Research Laboratory, TRRL Laboratory Report 913, Crowthorne, Berkshire, UK, 1980.

[9] P. M. Watson, "Features of the Experimental Safety Motorcycle ESM1," in *Seventh International Technical Conference on Experimental Safety Vehicles (ESV)*, Paris, France, 1979.

[10] T. Kuroe, H. Namiki and S. Iijima, "Exploratory study if an airbag concept for a large touring motorcycle: further research second report," in *The 19th International Technical Conference on the Enhanced Safety of Vehicles (ESV)*, Washington, DC, USA, 2005.

[11] H. Van Driessche, "Development of an ISO Standard for Motorcycle Research Impact Test Procedures," in *The Fourteenth International Technical Conference on Enhanced Safety of Vehicles (ESV)*, Munich, Germany, 1994.

[12] J. A. Newman, J. W. Zellner and K. D. Wiley, "A Motorcyclist Anthropometric Test Device MATD," in *IRCOBI Conference*, Berlin, Germany, 1991.

[13] A. Chawla and S. Mukherjee, "Motorcycle safety device investigation: A case study on airbags," *Sadhana,* vol. 32, no. 4, pp. 427-443, 2007.

[14] F. A. Berg, H. Burkle, F. Schmidts and J. Epple, “Analysis of the passive safety of motorcycles using accident investigations and crash tests,” in *The sixteenth International Technical Conference on the Enhanced Safety of Vehicles (ESV)*, Windsor, Ontario, Canada, 1998.

[15] H. H. Hurt, J. V. Ouellet and D. R. Thorn, “Final Report-Motorcycle Accident Cause Factors and Identification of Countermeasures,” U.S. Department of Transportation, National Highway Traffic Safety Administration; DOT HS-5-01160, 1981.

[16] ACEM, “MAIDS Final Report,” ACEM (European Motorcycle Manufacturers Association), Brussels, 2009.

[17] A. Grassi, N. Baldanzini, D. Barbani and M. Pierini, “A comparative analysis of MAIDS and ISO13232 databases for the identification of the most representative impact scenarios for powered 2-wheelers in Europe,” *Traffic Injury Prevention,* vol. 19, no. 7, pp. 766-772, 2018.

[18] G. Mensa, S. Piantini, N. Baldanzini, M. del Mar Rasines, N. Parera, M. Pierini, M. Pieve, P. Zampieri and S. Fodera, “Guidelines for the policy making: Future trends in accident scenarios and ISO 132323 review,” PIONEERS Project Deliverable D1.3 [https://pioneers-project.eu/wp-content/uploads/2020/12/Deliverable-D1.3.pdf], 2019.

[19] P. Puthan, N. Lubbe, J. Shaikh, B. Sui and J. Davidsson, “Defining crash configurations for Powered Two-Wheelers: Comparing ISO 13232 to recent in-depth crash data from Germany, India and China,” *Accident Analysis and Prevention,* vol. 151, no. 2021, 2021.

[20] AAAM, The Abbreviated Injury Scale 2015 Revision, Chicago Illinois: AAAM (Association for the Advancement of Automotive Medicine), 2015.

[21] F. Gidion, J. Carroll and N. Lubbe, “Motorcyclist injuries: Analysis of German in-depth crash data to identify priorities for injury assessment and prevention,” *Accident Analysis and Prevention,* vol. 163, no. 2021, 2021.

[22] J. Carroll, F. Gidion, M. Rizzi and N. Lubbe, “Do motorcyclist injuries depend on motorcycle and crash types? An analysis based on the German In-Depth Accident Study,” in *International Motorcycle Conference*, Cologne, Germany, 2022.

[23] A. Preiss and H. Wirsching, “RAMSIS is facing the 20s. Golden 20s?,” in *RAMSIS User Conference*, 2020.

[24] L. Schneider, D. Robbins, M. Pflug and R. Snyder, “Development of Anthrompometrically based Design Spcifications for an Advanced Anthropometric Dummy Family,” University of Michigan Transportation Research Institute, 1983.

[25] D. Robbins, “Anthrompetric Specifications for a Mid-Sized Male Dummy,” University of Michigan Transportation Research Institute, 1983.

[26] H. Singh, C.-D. Kan, D. Marzougui, R. M. Morgan and S. Quong, “Update to future midsize lightweight vehicle findings in response to manufacturer revew and IIHS small-overlap testing. Report No. DOT HS 812 237,” National Highway Traffic Safety Administration (NHTSA) , Washington, D.C., 2016.

[27] B. Been, M. Philippens, R. de Lange and M. van Ratingen, “WorldSID Dummy Head-Neck Biofidelity Response,” *Stapp Car Crash Journal,* vol. 48, no. Paper number 2004-22-0019, pp. 431-454, 2004.

[28] J. Carroll, B. Been, H. Sundmark, M. Burleigh and B. Li, “A Powered Two-Wheeler Crash Test Dummy,” in *International Research Council on the Biomechanics of Injury (IRCOBI) Conference Proceedings*, Porto, Portugal, 2022.

[29] E. Hertz, “A note on the Head Injury Criterion (HIC) as a predictor of the risk of skull fracture,” in *37th Annual Proceedings of the Association for the Advancement of Automotive Medicine (AAAM)*, San Antonio, Texas, 1993.

[30] H. J. Mertz, A. Irwin and P. Prasad, “Biomechanical and Scaling Basis for Frontal and Side Impact Injury Assessment Reference Values,” in *Stapp Car Crash Journal*, The Stapp Association, 2016.

[31] H. J. Mertz, J. D. Horsch, G. Horn and R. W. Lowne, “Hybrid III Sternal Deflection Associated with Thoracic Injury Severities of Occupants Restrained with Force-Limiting Shoulder Belts,” *SAE 910812,* 1991.

APPENDIX

Time (s)	Physical test	Simulation
0.000		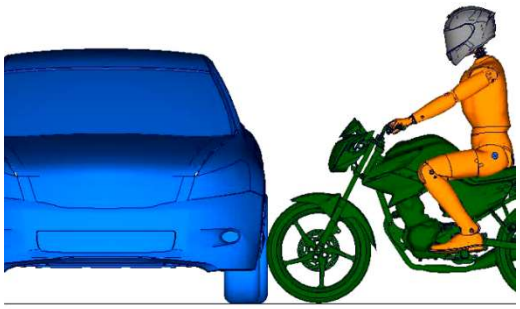
0.020		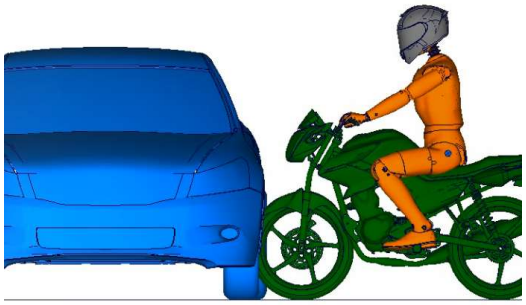
0.040		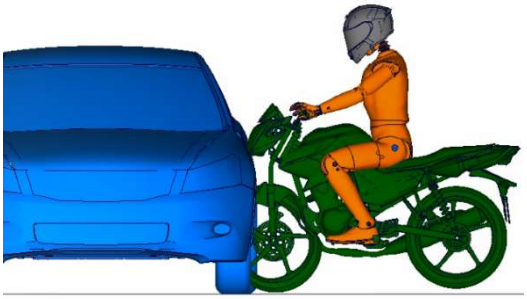
0.060		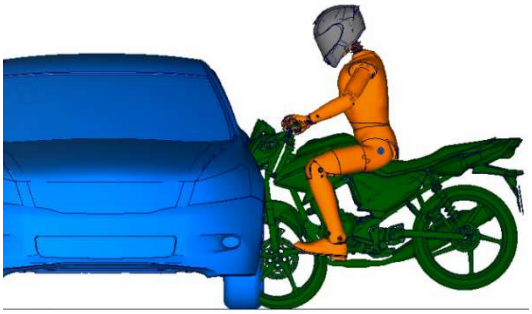
0.080		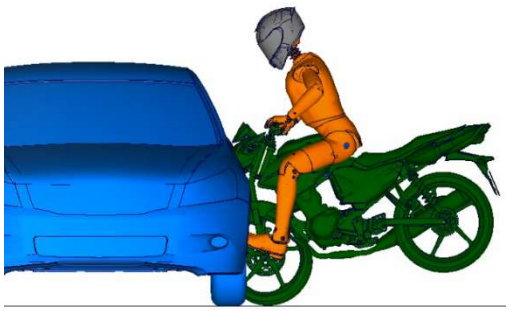

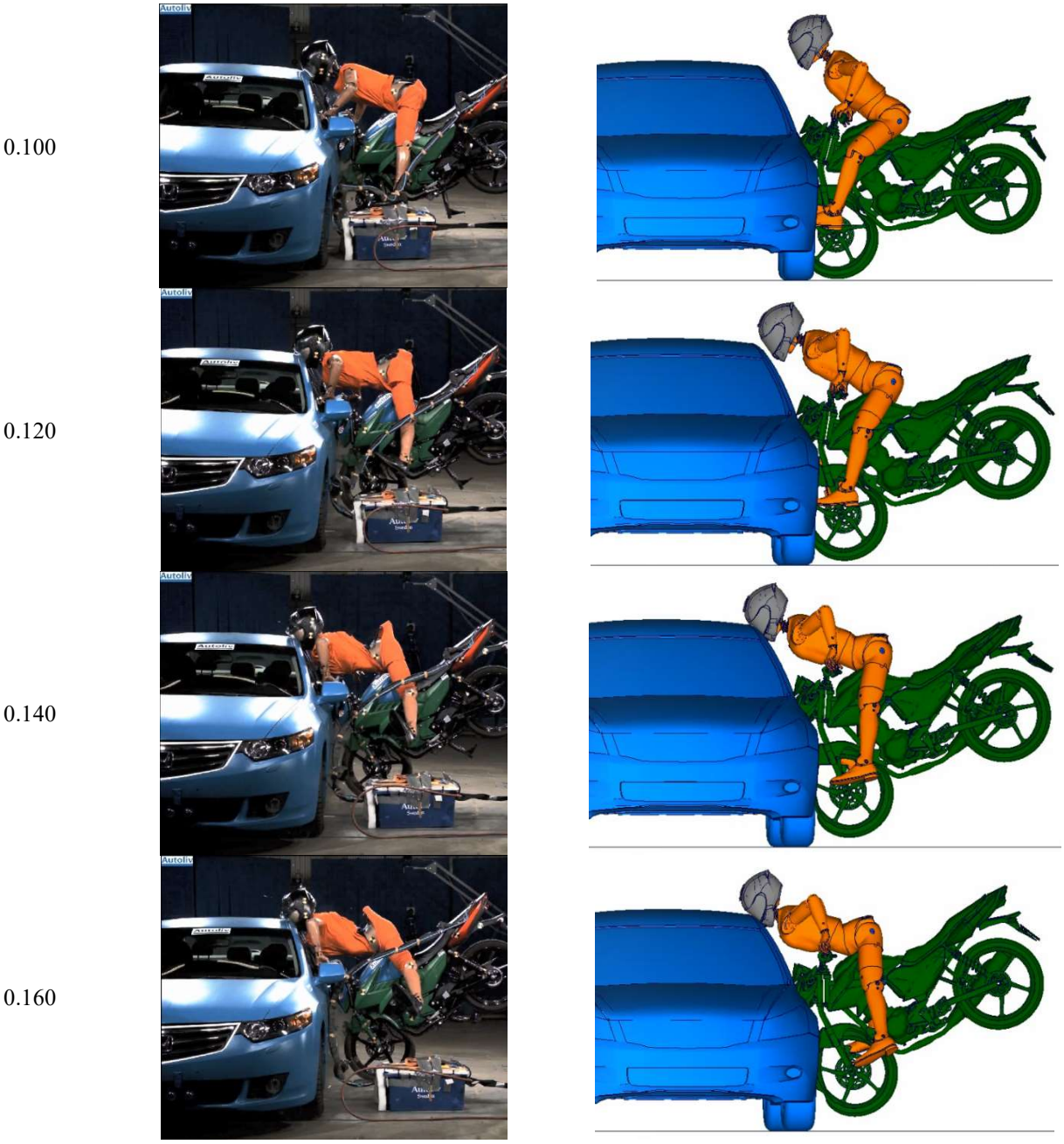

Figure 9. Still images from the videos of a full-scale motorcycle to stationary car crash test. The left-hand column of images comes from the physical test and the right-hand column of images from the finite-element simulation.

Time (s)	Physical test	Simulation
0.000	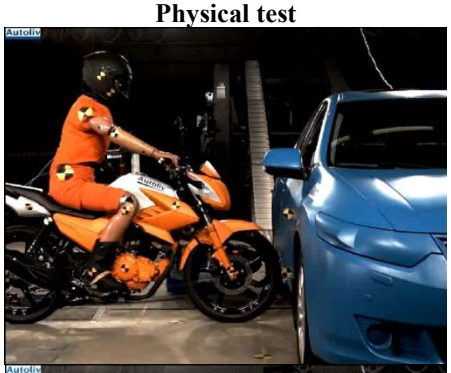	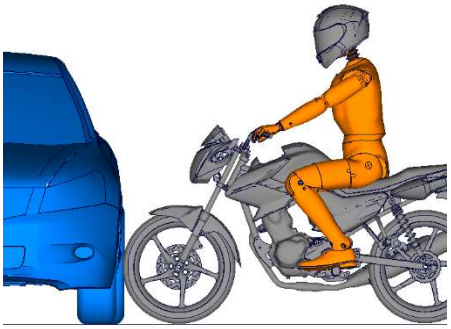
0.020		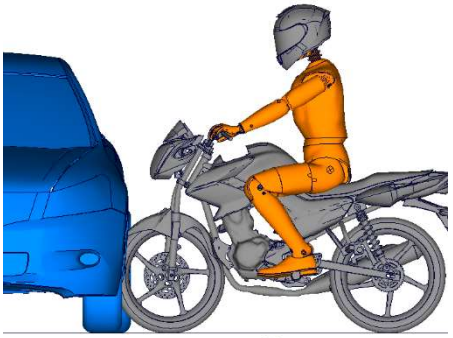
0.040		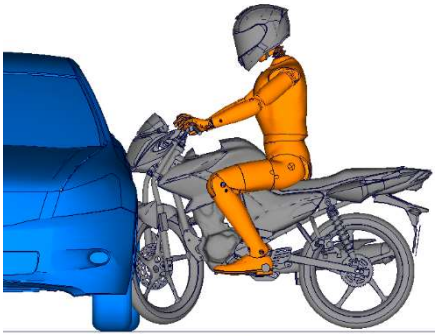
0.060		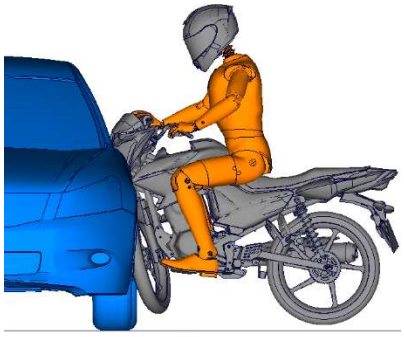
0.080		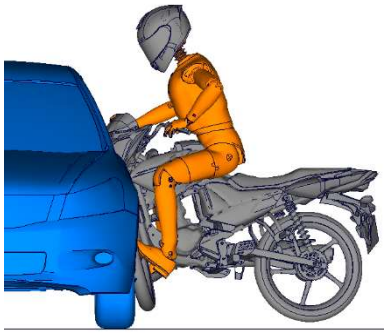

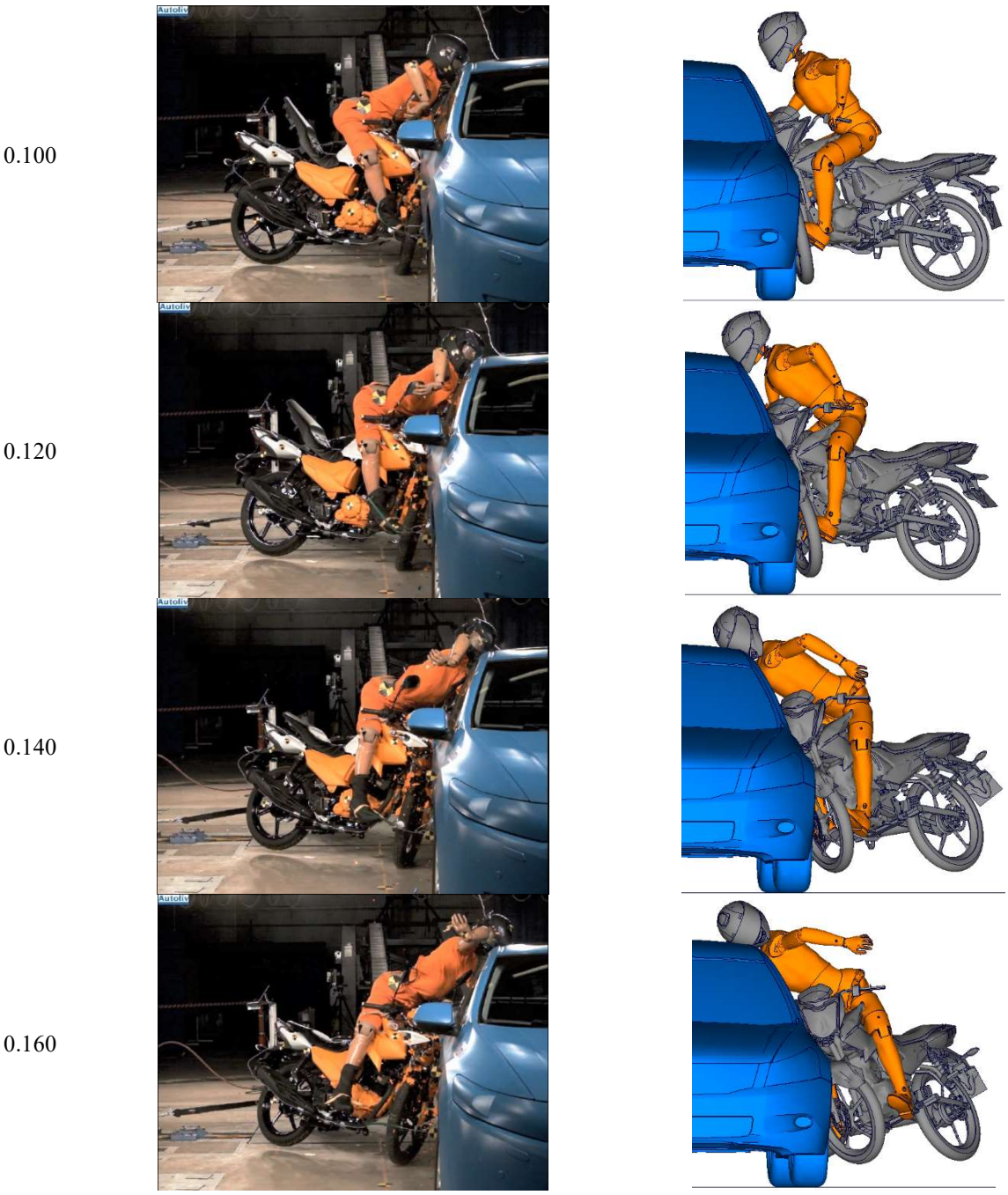

Figure 10. Still images from the videos of a full-scale motorcycle to moving car crash test. The left-hand column of images comes from the physical test and the right-hand column of images from the finite-element simulation.